

### A defined culture method enabling the establishment of ring sideroblasts from induced pluripotent cells of X-linked sideroblastic anemia

Congenital sideroblastic anemia is an inherited anemia characterized by the presence of bone marrow ring sideroblasts.<sup>1</sup> To date, several causative genes, mostly related to iron and heme metabolism in erythroid cells, have been considered critical for the formation of ring sideroblasts.<sup>1</sup> However, the biological characteristics of ring sideroblasts remain elusive because of the lack of an experimental model. We established culture conditions to induce ring sideroblasts *in vitro* based on induced pluripotent stem (iPS) cells derived from a patient with congenital sideroblastic anemia. To our knowledge, this is the first successful establishment of ring sideroblasts.

X-linked sideroblastic anemia (XLSA), the most common type of congenital sideroblastic anemia, is caused by defects in the X-linked gene encoding 5-aminolevulinic acid synthase 2 (*ALAS2*).<sup>1,2</sup> Most XLSA-associated mutations in *ALAS2* are missense substitutions that cause the loss of protein function, whereas mutations in the *ALAS2* regulatory region, which includes the promoter and intron 1,1 cause decreased *ALAS2* expression. Missense mutations commonly decrease the binding of *ALAS2* to pyridoxal 5'-phosphate (vitamin B6), a cofactor for the enzymatic activity of *ALAS2*, accounting for the responsiveness of patients with XLSA harboring such mutations to pyridoxal 5'-phosphate treatment.<sup>1</sup> However, approximately half of XLSA cases are unresponsive to pyridoxal 5'-phosphate,<sup>1,2</sup> necessitating the exploration of novel therapeutic strategies.

An *in vivo* model of XLSA is, therefore, needed to elucidate the underlying molecular mechanisms that contribute to the formation of ring sideroblasts and explore novel therapeutic strategies. However, *Alas2*-knockout mice die by day 11.5 *in utero* and are not, therefore, available for further testing.<sup>3</sup> Moreover, although ring sideroblast formation is observed after the transgenic rescue of *ALAS2* in *Alas2*-knockout mice, these mice die soon after birth.<sup>4</sup> Heme-deficient erythroblasts, derived from *Alas2*-knockout embryonic stem cells, through *in vitro* culture with OP9 cells, exhibited aberrant cytoplasmic iron accumulation but failed to present as typical ring sideroblasts.<sup>5</sup> These previous findings highlight the need for a model of XLSA.

Since the first report on iPS cells, various disease-specific human iPS cells have been established to partially recapitulate disease phenotypes.<sup>6</sup> However, while such iPS cell models have been established for hematologic disorders, no previous reports have described the establishment of an iPS cell model of XLSA. We, therefore, attempted to establish an iPS cell line from a patient with XLSA. The study protocol was approved by the Ethics Committee of Tohoku University Graduate School of Medicine. Clinical samples were collected after obtaining written informed consent.

A 14-year old male had exhibited microcytic anemia since childhood (Table 1). Bone marrow analysis revealed ring sideroblasts (50% of all erythroblasts) (*Online Supplementary Figure S1A*) with normal karyotype. The genetic analysis identified a thymine-to-cytosine substitution in exon 11 (T1737C) that caused a change in the 562nd amino acid of the *ALAS2* polypeptide from valine to alanine (Val562Ala) (*Online Supplementary Figure S1B*). The patient was diagnosed with XLSA and found to be responsive to vitamin B6. We established bone marrow mesenchymal stem cells from the patient's bone marrow sample (*Online Supplementary Figure S2*). The phenotype of these cells was confirmed based on morphology (*Online*

**Table 1.** Hematologic and biochemical data.

Hematological data		Normal range
White blood cells	3,800/ $\mu$ L	(4,000 - 9,000)
Neutrophils	34%	(28 - 68)
Lymphocytes	57%	(17 - 57)
Monocytes	4%	(0 - 10)
Eosinophils	4%	(0 - 10)
Basophils	1%	(0 - 2)
Red blood cells	450 x 10 <sup>9</sup> / $\mu$ L	(427 - 570 x 10 <sup>9</sup> )
Hemoglobin	<b>8.1 g/dL</b>	(14 - 18)
Mean corpuscular volume	<b>57.7 fL</b>	(80 - 100)
Mean corpuscular hemoglobin concentration	31.1%	(31 - 35)
Reticulocyte	<b>2.2%</b>	(0.7 - 2)
Platelets	<b>60.1 x 10<sup>9</sup>/<math>\mu</math>L</b>	(15 - 35 x 10 <sup>9</sup> )
Biochemical data		Normal range
Total protein	6.9 g/dL	(6.7-8.1)
Albumin	4.3 g/dL	(3.8-5.3)
Aspartate transaminase	14 U/L	(8-38)
Alanine transaminase	8 IU/L	(4-43)
Alkaline phosphatase	<b>979 IU/L</b>	(115-359)
Lactate dehydrogenase	155 IU/L	(119-229)
Gamma-glutamyltransferase	14 mg/dL	(10-47)
Total bilirubin	<b>1.6 mg/dL</b>	(0.2-1)
Blood urea nitrogen	11 mg/dL	(8-20)
Creatinine	0.5 mg/dL	(0.44-1.15)
C-reactive protein	0.1 mg/dL	(0-0.14)
Iron	242 g/dL	(54-181)
Total iron binding capacity	279 g/dL	(231-385)
Ferritin	<b>223 ng/mL</b>	(50-200)

Abnormal values are shown in bold.

*Supplementary Figure S2A*), differentiation potential into adipogenic/osteogenic lineages (*Online Supplementary Figure S2B*), and immunophenotypes (*Online Supplementary Figure S2C*). Additionally, Sanger sequencing confirmed *ALAS2* mutations in these mesenchymal stem cells (*Online Supplementary Figure S2D*). Similarly, we established bone marrow mesenchymal stem cells from a healthy donor.

The bone marrow mesenchymal stem cells derived from a healthy donor and the patient with XLSA were reprogrammed to iPS cells (termed NiPS and XiPS cells, respectively) using episomal vectors encoding OCT3/4, NANOG, SOX2, KLF4, L-MYC, LIN28, GLIS1, and shp53 (p53 shRNA) (*Online Supplementary Figure S3A*). One NiPS cell clone and one XiPS cell clone were selected for further characterization. G-band karyotype analysis confirmed normal karyotypes. Additionally, immunocytochemical staining of the iPS cell clones confirmed the expression of transcription factors OCT3/4 and NANOG and surface markers SSEA-4 and TRA-1-60, which are characteristic of human embryonic stem cells (*Online Supplementary Figure S3B*). Next, we confirmed the pluripotency of both NiPS and XiPS cells based on the spontaneous differentiation of embryoid bodies *in vitro* (*Online Supplementary Figure S4A*) and teratoma formation *in vivo* (*Online Supplementary Figure S4B*). No significant differences were observed between

XiPS and NiPS cells regarding iPS cell induction efficiency or characterization (*Online Supplementary Figures S3 and S4*). Furthermore, Sanger sequencing confirmed the presence of an *ALAS2* mutation in XiPS cells (Figure 1A).

Regarding the combination of reprogramming factors, introduction of LIN28, shp53, and GLIS1 in addition to the four originally reported factors (i.e., OCT3/4, SOX2, MYC, and KLF4) may enhance the efficiency of iPS cell establishment.<sup>7</sup> Here, we successfully and efficiently established

XLISA-iPS cells from bone marrow mesenchymal stem cells using a non-integrating episomal vector<sup>7</sup> encoding seven factors (i.e., OCT3/4, SOX2, KLF4, L-MYC, LIN28, GLIS1, and shp53). Transfection efficiency into bone marrow mesenchymal stem cells is not satisfactory,<sup>8</sup> but our approach could be applied to various cell types for establishing iPS cells.

Furthermore, co-culture of iPS cells with stromal cell lines has commonly been used to obtain erythroblasts from

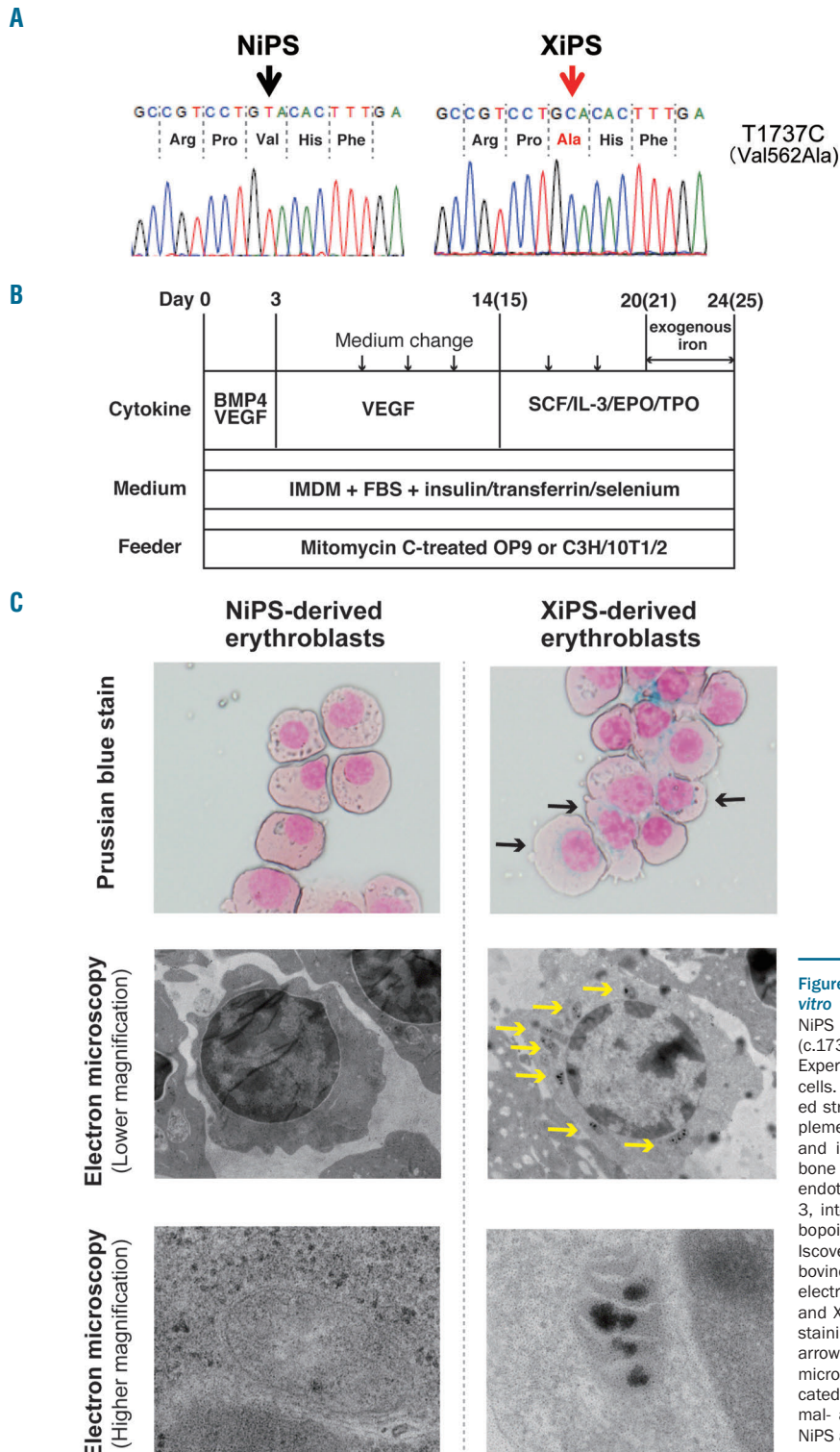


**Figure 1. Establishment of ring sideroblasts *in vitro* from XiPS cells.** (A) Sanger sequencing of NiPS and XiPS cells showing a T to C substitution (c.1737) in the *ALAS2* gene in XiPS cells. (B) Experimental protocol for co-culture with stromal cells. Cells were re-seeded onto mitomycin C-treated stromal cells on day 15; the medium was supplemented on day 21 with sodium ferrous citrate and incubated for an additional 4 days. BMP4, bone morphogenetic protein 4; VEGF, vascular endothelial growth factor; SCF, stem cell factor; IL-3, interleukin-3; EPO, erythropoietin; TPO, thrombopoietin; SFC, sodium ferrous citrate; IMDM, Iscove modified Dulbecco medium; FBS, fetal bovine serum. (C) Prussian blue staining (top) and electron microscopy (middle and bottom) of NiPS- and XiPS-derived erythroblasts. For Prussian blue staining, typical ring sideroblasts are indicated by arrows. For the lower magnification of electron microscopy, mitochondrial iron deposits are indicated by arrows. For the higher magnification, normal- and iron-loaded mitochondria, derived from NiPS and XiPS, respectively, are indicated.

iPS cells.<sup>9</sup> We, therefore, differentiated NiPS and XiPS cells into erythroid cells by co-culturing with stromal cells. iPS cells were seeded onto mitomycin C-treated stromal cells (OP9 or C3H/10T1/2; American Type Culture Collection, Manassas, VA, USA) with Iscove modified Dulbecco medium (IMDM; Life Technologies) supplemented with fetal bovine serum, insulin–transferrin–selenium, bone morphogenetic protein 4 (40 ng/mL), and vascular endothelial growth factor (20 ng/mL) (Figure 1B). On day 3, this medium was replaced with fresh IMDM (Sigma-Aldrich) supplemented with fetal bovine serum, insulin–transferrin–selenium, and vascular endothelial growth factor (20 ng/mL). On day 14 or 15, total cells were harvested, filtered (70 µm), and seeded onto mitomycin C-treated stromal cells with IMDM (Sigma-Aldrich) supplemented this time with fetal bovine serum, insulin–transferrin–selenium, stem cell factor (40 ng/mL), interleukin-3 (10 ng/mL), erythropoietin (3 IU/mL), and thrombopoietin (20 ng/mL). On day 20 or 21, the cell culture was supplemented with 250 µM sodium ferrous citrate and incubated for an additional 4 days. The number of erythroblasts decreased drastically by day 28, so the cells were harvested by day 25.

Interestingly, approximately 20% of erythroblasts obtained from XiPS cells exhibited ring sideroblasts and abnormal iron deposition in the mitochondria, as confirmed by electron microscopy (Figure 1C); without the addition of sodium ferrous citrate, obvious ring sideroblast formation was not confirmed. Prolonged exposure (>5 days) or higher concentrations of exogenous iron (>250 µM) did not increase the proportion of ring sideroblasts (*data not shown*). On the other hand, abnormal iron deposition was not detected in NiPS cell-derived erythroblasts (Figure 1C). May-Giemsa staining of erythroblasts derived from XiPS and NiPS cells indicated orthochromatic stages of erythroblasts (Online Supplementary Figure S5), suggesting that erythroid differentiation was not compromised despite the *ALAS2* mutation in this *in vitro* system. In conjunction with the observation that ferritin clumps were present only in XiPS cell-derived erythroblasts (Figure 1C, lower magnification), we anticipate that defective iron utilization in *ALAS2*-mutated erythroblasts may result not only in mitochondrial iron overload, but also in the emergence of ferritin clumps as a consequence of cellular iron overload. In support of our hypothesis, we have demonstrated that *Alas2*-null murine definitive erythroblasts contain ferritin aggregates in the cytosol.<sup>5</sup> Because our patient with XLSA was responsive to vitamin B6, supplementing the culture media with vitamin B6 may partially restore the compromised *ALAS2* activity enabling iron to be used correctly. However, the differentiation of XiPS cells with vitamin B6-depleted IMDM medium did not induce ring sideroblasts (*data not shown*). It is anticipated that HCl pyridoxal supplementation of IMDM would be insufficient to improve the enzymatic activity of the *ALAS2* Val562Ala mutant.

Initially, we applied a serum-free monolayer culture with the stepwise tuning of exogenous cytokine cocktails.<sup>11</sup> While this protocol has several advantages, including a simple culture method without the need for stromal cells and easy traceability of morphological changes,<sup>11</sup> erythroblasts derived from XiPS cells did not exhibit ring sideroblasts. Although the reason remains unknown, we speculate that stromal cells may promote erythroid differentiation in XiPS cells with the additional secreted factors from the stromal cells or the signals delivered through adhesion molecules.

Besides the *ALAS2* mutation, a series of factors critical for the formation of ring sideroblasts have been elucidated, including the mutation of genes involved in heme biosyn-

thesis (e.g., *SLC25A38* and *FECH*), iron–sulfur cluster biogenesis (e.g., *ABCB7*, *GLRX5*, and *HSPA9*), mitochondrial protein synthesis (e.g., *TRNT1*, *YARS2*, *PUS1*, *SLC19A2*, *NDUFV11*, and mitochondrial DNA), and RNA splicing machinery (e.g., *SF3B1*).<sup>11–13</sup> Recently, one report on iPS cells from a patient with a mitochondrial deletion/Pearson syndrome implicated the formation of ring sideroblasts; however, this was not confirmed with electron microscopy.<sup>14</sup> No effective treatment has been established for sideroblastic anemia not related to the *ALAS2* mutation, but our defined culture protocol would lead to better understanding of the pathophysiology of both congenital and acquired sideroblastic anemias.

To the best of our knowledge, no previous report has described the establishment of ring sideroblasts through *in vitro* culture. One potential limitation of the present protocol is that only a subset of the XiPS cell-derived erythroblasts (approximately 20%) exhibited ring sideroblasts, a problem which may be overcome by establishing an immortalized erythroblast clone with ring sideroblasts based on viral transduction of the hematopoietic transcription factor TAL1 and human papillomavirus type 16-E6/E7.<sup>15</sup> Nevertheless, further phenotypic analyses of ring sideroblasts could lead to a better understanding of the molecular basis of XLSA and the establishment of novel therapeutic strategies.

Shunsuke Hatta,<sup>1,2</sup> Tohru Fujiwara,<sup>1</sup> Takako Yamamoto,<sup>3</sup> Kei Saito,<sup>1</sup> Mayumi Kamata,<sup>1</sup> Yoshiko Tamai,<sup>3</sup> Shin Kawamata<sup>1</sup> and Hideo Harigae<sup>1</sup>

<sup>1</sup>Department of Hematology and Rheumatology, Tohoku University Graduate School of Medicine, Sendai; <sup>2</sup>Division of Cell Therapy, Foundation of Biomedical Research and Innovation, Kobe and <sup>3</sup>Department of Gastroenterology and Hematology, Hirosaki University Graduate School of Medicine, Japan

*Acknowledgments:* we thank Dr. Ryo Ichinohasama (Tohoku University) for helpful comments regarding the histological examination and Ms. Kumiko An (Tohoku University Hospital) for conducting the G-band analysis. We also thank Dr. Okeita (Center for iPS Cell Research and Application, Kyoto University, Kyoto, Japan) for kindly providing the episomal vectors. Furthermore, we acknowledge the support of Biomedical Research Core of Tohoku University School of Medicine.

*Funding:* this work was supported by JSPS KAKENHI Grant Number 16K19564 to SH.

*Correspondence:* harigae@med.tohoku.ac.jp  
doi:10.3324/haematol.2017.179770

*Information on authorship, contributions, and financial & other disclosures was provided by the authors and is available with the online version of this article at www.haematologica.org.*

## References

- Bottomley SS, Fleming MD. Sideroblastic anemia: diagnosis and management. *Hematol Oncol Clin North Am.* 2014;28(4):653–670.
- Ohba R, Furuyama K, Yoshida K, et al. Clinical and genetic characteristics of congenital sideroblastic anemia: comparison with myelodysplastic syndrome with ring sideroblast (MDS-RS). *Ann Hematol.* 2013;92(1):1–9.
- Nakajima O, Takahashi S, Harigae H, et al. Heme deficiency in erythroid lineage causes differentiation arrest and cytoplasmic iron overload. *EMBO J.* 1999;18(22):6282–6289.
- Nakajima O, Okano S, Harada H, et al. Transgenic rescue of erythroid 5-aminolevulinic synthase-deficient mice results in the formation of ring sideroblasts and siderocytes. *Genes Cells.* 2006;11(6):685–700.
- Harigae H, Nakajima O, Suwabe N, et al. Aberrant iron accumulation and oxidized status of erythroid-specific delta-aminolevulinic synthase (*ALAS2*)-deficient definitive erythroblasts. *Blood.* 2003;101(3):1188–1193.

6. Takahashi K, Yamanaka S. Induction of pluripotent stem cells from mouse embryonic and adult fibroblast cultures by defined factors. *Cell*. 2006;126(4):663-676.
7. Okita K, Yamakawa T, Matsumura Y, et al. An efficient nonviral method to generate integration-free human-induced pluripotent stem cells from cord blood and peripheral blood cells. *Stem Cells*. 2013;31(3):458-466.
8. Kanehira M, Fujiwara T, Nakajima S, et al. An lysophosphatidic acid receptors 1 and 3 axis governs cellular senescence of mesenchymal stromal cells and promotes growth and vascularization of multiple myeloma. *Stem Cells*. 2017;35(3):739-753.
9. Lapillonne H, Kobari L, Mazurier C, et al. Red blood cell generation from human induced pluripotent stem cells: Perspectives for transfusion medicine. *Haematologica*. 2010;95(10):1651-1659.
10. Niwa A, Heike T, Umeda K, et al. A novel serum-free monolayer culture for orderly hematopoietic differentiation of human pluripotent cells via mesodermal progenitors. *PLoS One*. 2011;6(7):e22261.
11. Cazzola M, Malcovati L. Diagnosis and treatment of sideroblastic anemias: from defective heme synthesis to abnormal RNA splicing. *Hematology Am Soc Hematol Educ Program*. 2015;2015:19-25.
12. Schmitz-Abe K, Ciesielski SJ, Schmidt PJ, et al. Congenital sideroblastic anemia due to mutations in the mitochondrial HSP70 homologue HSPA9. *Blood*. 2015;126(25):2734-2738.
13. Guemsey DL, Jiang H, Campagna DR, et al. Mutations in mitochondrial carrier family gene SLC25A38 cause nonsyndromic autosomal recessive congenital sideroblastic anemia. *Nat Genet*. 2009;41(6):651-653.
14. Cherry AB, Gagne KE, McLoughlin EM, et al. Induced pluripotent stem cells with a mitochondrial DNA deletion. *Stem Cells*. 2013;31(7):1287-1297.
15. Kurita R, Suda N, Sudo K, et al. Establishment of immortalized human erythroid progenitor cell lines able to produce enucleated red blood cells. *PLoS One*. 2013;8(3):e59890.